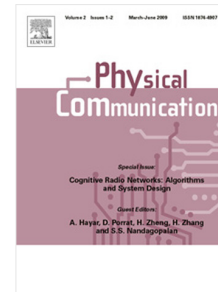


Accepted Manuscript

A novel bandwidth and power allocation scheme for power efficient hybrid RF/VLC indoor systems

Mai Kafafy, Yasmine Fahmy, Mohamed Abdallah, Mohamed Khairy



PII: S1874-4907(17)30589-X

DOI: <https://doi.org/10.1016/j.phycom.2018.04.025>

Reference: PHYCOM 543

To appear in: *Physical Communication*

Received date: 12 December 2017

Revised date: 29 March 2018

Accepted date: 30 April 2018

Please cite this article as: M. Kafafy, Y. Fahmy, M. Abdallah, M. Khairy, A novel bandwidth and power allocation scheme for power efficient hybrid RF/VLC indoor systems, *Physical Communication* (2018), <https://doi.org/10.1016/j.phycom.2018.04.025>

This is a PDF file of an unedited manuscript that has been accepted for publication. As a service to our customers we are providing this early version of the manuscript. The manuscript will undergo copyediting, typesetting, and review of the resulting proof before it is published in its final form. Please note that during the production process errors may be discovered which could affect the content, and all legal disclaimers that apply to the journal pertain.

A Novel Bandwidth and Power Allocation Scheme for Power Efficient Hybrid RF/VLC Indoor Systems

Mai Kafafy^{a,*}, Yasmine Fahmy^a, Mohamed Abdallah^b, Mohamed Khairy^a

^a *Electronics and Communications Engineering Department, Cairo University, Giza, Egypt, 12613*

^b *College of Science and Engineering, Hamad Bin Khalifa University, Doha, Qatar*

Abstract

Indoor Visible Light Communication (VLC) uses the illumination power of indoor LED luminaries for data transmission. Deploying RF communication alongside VLC is preferable as it improves the coverage and the reliability of the system. This paper studies the power efficiency of hybrid RF/VLC indoor systems. The power efficiency is defined as the system's total rate per unit power consumed, and the paper considers a hybrid system consisting of a single RF access point and multiple interfering VLC access points. We develop a joint power and bandwidth allocation scheme that iteratively optimizes the power and bandwidth allocated by the access points to their associated users to maximize the system's power efficiency. We compare the power efficiency of the hybrid system for different layouts of the VLC access points, and we show through simulations that deploying VLC alongside RF communication improves the power efficiency of the hybrid system, especially when users receive low RF signal due to walls.

Keywords: indoor visible light communication, resource allocation, power efficiency, hybrid RF/VLC networks

*Corresponding author

Email addresses: mai.b.s.ali@eng.cu.edu.eg (Mai Kafafy), yfahmy@cws-cufe.org (Yasmine Fahmy), moabdallah@hkbu.edu.qa (Mohamed Abdallah), mkhairy@ieee.org (Mohamed Khairy)

1. Introduction

The growing trend towards energy efficient communication and the recent progress in solid state lighting technology [1] promote the deployment of Visible Light Communication (VLC) in indoor systems. VLC systems convey information through optical radiation in the visible light spectrum band (375nm-780nm) [2]. The modulation and demodulation techniques used in VLC are called intensity modulation and direct detection [3]. A VLC transmitter modulates the intensity of the output visible light of a Light Emitting Diode (LED) device, and a VLC receiver uses a photo detector to detect the received optical signal.

The intensity of the LEDs output light should be modulated at a rate higher than the flicker rate of the eye in order to be unnoticeable to the human eye [4].

VLC is a promising candidate technology for indoor communication in future 5G networks [5, 6] for the following reasons. It operates on a wide unlicensed spectrum band that can be reused in different rooms without inter room interference due to the confinement of visible light between walls. VLC is secure and it is a safe technology that can be used in places where Radio Frequency (RF) communication is not preferred or even allowed like airplanes and hospitals. VLC uses the illumination power of LED devices for communication purposes which offers power efficient solutions especially in places like offices and conference or lecture rooms where the lights are always on.

Deploying VLC in conjunction with RF communication is preferable for the following reasons. VLC is prone to performance degradation when obstacles and passing objects interrupt the Line of Sight (LoS) between the transmitter and the receiver, and therefore hybrid RF/VLC systems offer better coverage and reliability. RF is also preferred to VLC in uplink channels to avoid undesired irradiance from mobile devices [7],[8]. Finally, VLC has zero RF interference and therefore the integration of the two technologies should not be problematic. The challenges of integrating RF with VLC are discussed in [9, 10]. Challenges include users' mobility and its effect on channel estimation and handover. Some challenges are represented in the effect of splitting traffic between the two sys-

tems and handling packet drop on upper layer protocols. Other challenges include channel aggregation and frequency reuse, and the back-hauling of VLC Access Points (APs).

Many papers investigated the performance of VLC systems [11–19]. Fewer references considered hybrid RF/VLC systems, and they mainly discussed load balancing [20–23], handover and network association[24–27], and rate and outage analysis [28, 29]. Even fewer references addressed the power efficiency of VLC and hybrid RF/VLC systems although it is an important topic due to the increasing energy consumption of the communication systems [30, 31], and the fact that most data is generated indoors [32]. Most of these references considered a simple system model consisting of a single VLC AP (or link), and therefore interference between VLC APs was not considered in their problem formulation. For example, paper [33] optimized power allocation to maximize the power efficiency of a SISO/MISO VLC only system that consists of a single VLC transmitter and a single VLC receiver. Paper [34] optimized power and bandwidth allocation to maximize the power efficiency of a hybrid RF/VLC system. The paper showed that a hybrid RF/VLC system has a higher power efficiency (defined as the total rate per unit power consumed) than an RF only system. But it only considered a simple system consisting of a single RF AP and a single VLC AP. Reference [35] minimized the transmission power of a simple hybrid RF/VLC system consisting of a single RF link and a single VLC link with power line communication as a communication backbone for VLC. Reference [36] optimized power allocation to maximize the power efficiency of a VLC only system consisting of multiple VLC cells. In order to simplify the problem, the paper removed the coupling between power allocation and the generated interference by considering the worst case interference when all the cells transmit with their maximum power.

The promising results in [34] encouraged us to extend their work to a more realistic indoor setting in this paper. We consider a room with a number of LED luminaries installed on the ceiling and working as VLC APs alongside an RF AP that is located outside the room. This model is valid for many sce-

narios. Examples include offices where the received RF signal is weak due to wall separation or in hospitals where RF APs are not allowed near the patients' rooms due to health concerns. The VLC APs use the same band, so VLC interference between VLC APs is present. We believe that ignoring the effect of power allocation on the generated interference is an unrealistic assumption because each AP should consider how the power it allocates to its associated users affects the rest of the users in the system. Therefore we do not make simplifying assumptions about the interference, and we keep the VLC interference term in our problem formulation as is (i.e., a function of the power allocation) which makes the problem more complex. We compare the power efficiency of the hybrid system for different number and different layouts of the deployed VLC APs.

In this paper, we consider the downlink of a hybrid RF/VLC indoor system consisting of one RF AP working in conjunction with multiple interfering VLC APs for serving a number of users. Our aim is to maximize the system power efficiency, defined as the users' sum rate divided by the total power consumed by the system. The total power consumed by the system is the RF transmission power and the power used for VLC data communications. The system's QoS is controlled through the minimum rate required by each user. We propose a joint locally optimal bandwidth and power allocation algorithm (JOBPA) that iteratively optimizes the power and bandwidth allocated by the RF and VLC APs to their associated users. We also compare the power efficiency for different numbers and layouts of the deployed VLC APs.

Simulations show that deploying VLC APs alongside the RF system improves the power efficiency due to spectrum reuse. The VLC system has the major contribution to the hybrid achieved rate, especially when the system has few users or relaxed QoS conditions. When the number of users increase or the minimum rate required increases, the RF system starts to be in operation.

The rest of this paper is organized as follows: section 2 describes our system model, and section 3 formulates the power efficiency maximization problem. Section 4 introduces our JOBPA algorithm. Section 5 describes our simula-

tion setup and shows the numerical results of the power efficiency achieved for different layouts of the VLC APs. Finally, section 6 concludes the paper.

⁹⁵ **2. System Model**

We consider the downlink of a hybrid RF/VLC network consisting of one RF AP working in conjunction with multiple interfering VLC APs to serve a number of users. We focus our attention on a typical room with a set V of downwards pointing luminaries installed on the ceiling. Each luminary consists ¹⁰⁰ of a number N_{LED} of LEDs, and has the potential of working as a VLC AP. The LED DC bias current (I_{DC}) and the number of LED per luminary (N_{LED}) are chosen to maintain specific illumination requirement in the room. The symbols I_{min} and I_{max} denote the minimum and maximum allowed LED driving currents, respectively. Each VLC AP serves its users orthogonally using Frequency ¹⁰⁵ Division Multiple Access (FDMA) (no interference between users of the same AP), and the VLC system has frequency reuse of one (i.e., all the VLC APs operate on the same frequency band). Finally, we denote the VLC bandwidth as $B_{VLC,max}$.

An RF AP is located outside the room of interest and therefore is separated ¹¹⁰ from the room by at least one wall. We believe that placing the RF AP outside the considered room is an acceptable assumption since many offices and/or classrooms receive weak signal from the RF AP serving the building or the floor in which they are located. Also, places like hospitals may require the RF AP to be placed far from the patients' rooms due to health concerns. We assume ¹¹⁵ that the RF AP has a maximum transmission power $P_{RF,max}$, and a bandwidth $B_{RF,max}$. The RF AP serves its associated users orthogonally using FDMA.

A set M of Mobile Terminals (MTs) is located randomly in the considered room, with each MT equipped with an RF receiver and a VLC receiver. Each MT has multi-homing capability such that a typical $MT-m$ ($m \in M$) is served ¹²⁰ by the RF AP and by the VLC AP- $s(m)$ with the maximum received signal strength (the nearest VLC AP). A central entity in the system architecture is

assumed to be responsible for the coordination between the RF AP and the VLC APs. The set of users served by VLC $AP-i$ is denoted by A_i . The cardinality of any set is denoted by $|\cdot|$ (e.g., $|A_i|$ is the number of MTs served by VLC $AP-i$).
125

Figure 1 is an example of a typical room with 9 luminaries installed on the ceiling. An RF AP is positioned outside the room. Two MTs at different heights (one with a standing person and one with a sitting person) are located in the room. Each MT is associated to its nearest VLC AP, and the two MTs
130 receive coverage from the RF AP. The white solid links represent the VLC link between the MTs and their serving VLC APs, and the black solid link represent the RF link between the MTs and the RF AP. The dashed arrows represent the interference observed by each MT from the neighbour VLC APs.

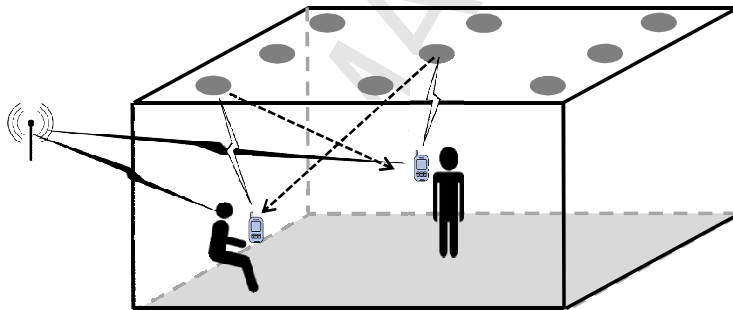


Figure 1: room model

2.1. RF Channel Gain

We consider the WINNER II channel model for an indoor office environment
135 [37]. The path loss from the RF AP to user $MT-m$ is

$$PL_m[\text{dB}] = A \log_{10}(d_{RF,m}) + B + C \log_{10}(f_c/5) + X, \quad (1)$$

where f_c is the carrier frequency in GHz, and $d_{RF,m}$ is the distance between $MT-m$ and the RF AP. For the non-Line of sight scenario, $A = 36.8$, $B = 43.8$, $C = 20$. $X = 12(n_w - 1)$ in case of heavy walls, where n_w is the number of
140

¹⁴⁰ walls between the AP and the MT. The RF large channel gain between the RF AP and $MT-m$ is calculated as follows

$$G_{RF,m} = 10^{-PL_m[\text{dB}]/10}. \quad (2)$$

2.2. VLC Channel Gain

¹⁴⁵ VLC channels have a LoS component resulting from the direct light propagation from the transmitter to the receiver, and diffuse components resulting from the light reflections. The energy of diffuse components are much lower than the energy of the LoS component, and are neglected in indoor VLC settings [38],[39]. Therefore, We only consider the LoS component of the optical VLC channel [40] between VLC $AP-i$ and $MT-m$, which is given by

$$g_{i,m}^{VLC} = N_{LED} \frac{(n+1) \cos^n(\phi_{i,m}) a_m \cos(\theta_{i,m})}{2\pi d_{i,m}^2} \text{rect}\left(\frac{\theta_{i,m}}{\text{FoV}}\right), \quad (3)$$

¹⁵⁰ where $n = \frac{\ln(1/2)}{\ln(\cos(\Phi))}$ is the order of the Lambertian emission, and Φ is the LED semi-angle at half power. The two angles $\phi_{i,m}$ and $\theta_{i,m}$ are the irradiance and the incidence angles between $AP-i$ and $MT-m$, respectively, and $d_{i,m}$ is the distance between $AP-i$ and $MT-m$. FoV is the receiver's field of view, and a_m is the physical area of the photo detector at $MT-m$.

3. Maximization of the System's Power Efficiency

¹⁵⁵ In this section, we formulate the power and bandwidth allocation problem of the hybrid RF/VLC system described in section 2 as an optimization problem. The objective to be maximized is the power efficiency of the system, defined as the users' sum rate (in bps) divided by the total power consumed (in Watt). The total power consumed by the system is the total transmission power of the ¹⁶⁰ RF AP (P_{RF}) added to the total electrical power dedicated to VLC communications. The power resulting from the LED DC bias current is not included in the calculations of the system's total consumed power because it is already used by the LED device for the illumination purposes.

The optimization problem is formulated in (4), where $P_{RF,m}$ and $B_{RF,m}$ are the RF power and bandwidth allocated to $MT-m$, respectively. $P_{VLC,m}$ and $B_{VLC,m}$ are the electrical power and bandwidth allocated to $MT-m$ by its serving VLC AP.

$$\max_{\substack{\{P_{RF,m}, B_{RF,m}, P_{VLC,m}, B_{VLC,m}\} \\ \forall m \in M}} \frac{\sum_{m \in M} (R_{RF,m} + R_{VLC,m})}{\sum_{m \in M} P_{RF,m} + N_{LED} \sum_{i \in V} \sum_{m \in A_i} P_{VLC,m}},$$

subject to

$$\begin{aligned} C1: \quad & \sum_{m \in M} P_{RF,m} \leq P_{RF,max}, \\ C2: \quad & \sum_{m \in A_i} P_{VLC,m} \leq P_{VLC,max}, \quad \forall i \in V, \\ C3: \quad & I_{DC} - \sqrt{P_{VLC,m}} \geq I_{min}, \quad \forall m \in A_i, i \in V \\ C4: \quad & I_{DC} + \sqrt{P_{VLC,m}} \leq I_{max}, \quad \forall m \in A_i, i \in V \\ C5: \quad & \sum_{m \in M} B_{RF,m} \leq B_{RF,max}, \\ C6: \quad & \sum_{m \in A_i} B_{VLC,m} \leq B_{VLC,max}, \quad \forall i \in V, \\ C7: \quad & R_{RF,m} + R_{VLC,m} \geq R_{min}, \quad \forall m \in M. \end{aligned} \tag{4}$$

Constraint C1 limits the total transmission power of the RF AP to P_{RF} . Constraint C2 limits the power budget of the VLC communication of each LED to $P_{VLC,max}$. Constraints C3 and C4 ensure that the driving current of each LED lies between I_{min} and I_{max} (all the LEDs operate at the same bias DC current I_{DC}). Constraints C5 and C6 limit the total bandwidth allocated by the RF AP and each VLC AP to $B_{RF,max}$ and $B_{VLC,max}$ respectively. Constraint C7 sets the minimum rate required by each MT, where $R_{RF,m}$ is the RF rate achieved by $MT-m$, and is given by

$$R_{RF,m} = B_{RF,m} \log_2 \left(1 + \frac{P_{RF,m} G_{RF,m}}{N_{oRF} B_{RF,m}} \right), \tag{5}$$

where $N_{oRF} = K_b T$ is the thermal noise power spectral density. K_b is the Boltzmann constant, and T is the ambient temperature [11]. The VLC rate

achieved by $MT\text{-}m$ from its serving VLC AP- $s(m)$ is [41]

$$R_{VLC,m} = \frac{B_{VLC,m}}{2} \log_2 \left(1 + \frac{P_{VLC,m} G_{VLC,m}}{No^{VLC} B_{VLC,m} + \Psi_m} \right), \quad (6)$$

where, $\Psi_m = \sum_{\substack{j \in V \\ j \neq s(m)}} \frac{G_{j,m}}{|A_j|} \sum_{l \in A_j} P_{VLC,l}$

180

where $G_{i,m} = (k\rho g_{i,m}^{VLC})^2$. k is the electrical to optical conversion efficiency of the LED in W/A, and ρ is the responsivity of the photo detector in A/W. Ψ_m is the downlink inter AP interference (IAPI) seen by $MT\text{-}m$. No^{VLC} is the shot noise power spectral density (in W/Hz), which is considered the dominant component [11], and is given by [42] as follows

$$No^{VLC} = 2qI_{bg}, \quad (7)$$

where q is the electron charge, and I_{bg} is the current from background light.

The optimization problem in (4) is non concave, and therefore is hard to be solved directly. In the next section, we develop a joint bandwidth and power allocation algorithm (JOBPA) which jointly optimizes the power and bandwidth allocated by the RF and the VLC APs to their associated users.

4. Joint Locally Optimal Bandwidth and Power Allocation Algorithm (JOBPA)

The proposed algorithm solves the non concave optimization problem in (4) by solving a power allocation sub-problem and a bandwidth allocation sub-problem iteratively using alternating optimization [43] as illustrated in Fig. 2.

4.1. RF/VLC Power Allocation

In the power allocation sub-problem, we consider the bandwidth allocation to be known and solve for the optimal power allocation. The numerator of the fractional objective in (4) is non-concave due to the non-concavity of the VLC rates $R_{VLC,m}$. We use sequential fractional programming [44] which implies solving

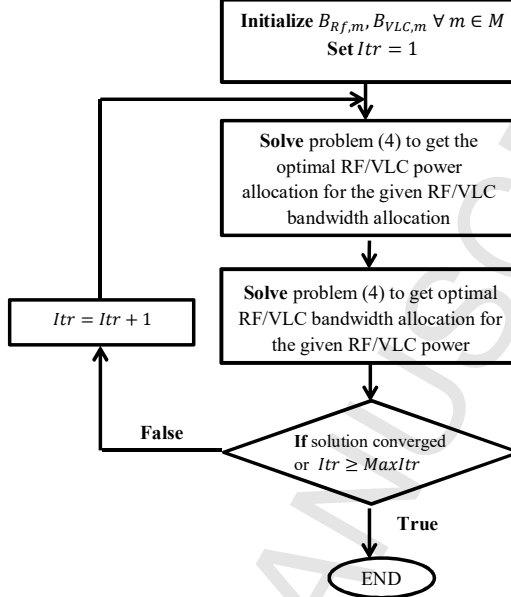


Figure 2: Flowchart of JOBPA

a sequence of concave over linear optimization problems using the Dinkelbach-Type algorithm [45]. Therefore, we reformulate the VLC rates $R_{VLC,m}$ as a difference between two log functions [46] with the second log approximated by its first order approximation around an arbitrary VLC power vector $\underline{P}_{VLC}^{(k)}$ as follows

$$R_{VLC,m}^{(k)} = \frac{B_{VLC,m}}{2} \left[\log_2(No^{VLC} B_{VLC,m} + P_{VLC,m} G_{s(m),m} + \Psi_m) - \gamma_m(\underline{P}_{VLC}^{(k)}) - \nabla_{\underline{P}_{VLC}^{(k)}}^T(\gamma_m)(\underline{P}_{VLC} - \underline{P}_{VLC}^{(k)}) \right], \quad (8)$$

where $\gamma_m = \log_2(No^{VLC} B_{VLC,m} + \Psi_m)$.

Replacing the VLC rates with their concave approximation in (8) makes the objective in (4) concave over linear. It can be put in the concave parametric form $\sum_{m \in M} (R_{RF,m} + R_{VLC,m}^{(k)}) - \lambda(\sum_{m \in M} P_{RF,m} + N_{LED} \sum_{i \in V} \sum_{m \in A_i} P_{VLC,m})$ [47], where the optimal solution is obtained by finding the roots of $F(\lambda) = 0$ in (9). The value of the parameter λ is updated using the Dinkelbach-Type algorithm [45].

$$\begin{aligned}
 F(\lambda) = \max_{\substack{\{P_{RF,m}, P_{VLC,m}\} \\ \forall m \in M}} & \left(\sum_{m \in M} (R_{RF,m} + R_{VLC,m}^{(k)}) \right. \\
 & \left. - \lambda \left(\sum_{m \in M} P_{RF,m} + N_{LED} \sum_{i \in V} \sum_{m \in A_i} P_{VLC,m} \right) \right) \\
 \text{subject to} \\
 \sum_{m \in M} P_{RF,m} & \leq P_{RF,max}, \\
 \sum_{m \in A_i} P_{VLC,m} & \leq P_{VLC,max}, \quad \forall i \in V, \\
 P_{VLC,m} & \leq P_{max}, \quad \forall m \in M, \\
 R_{RF,m} + R_{VLC,m}^{(k)} & \geq R_{min}, \quad \forall m \in M,
 \end{aligned} \tag{9}$$

215 where $P_{max} = \min[(I_{DC} - I_{min})^2, (I_{max} - I_{DC})^2]$. The optimization problem in (9) is concave and can be solved using convex optimization software [48] or using the KKT conditions [49],[50]. The Lagrangian of the power allocation problem is

$$\begin{aligned}
 L = \sum_{m \in M} & \left(R_{RF,m} + R_{VLC,m}^{(k)} \right) - \lambda \left(\sum_{m \in M} P_{RF,m} + N_{LED} \sum_{i \in V} \sum_{m \in A_i} P_{VLC,m} \right) \\
 & + \beta^{RF} \left(P_{RF,max} - \sum_{m \in M} P_{RF,m} \right) + \sum_{i \in V} \beta_i \left(P_{VLC,max} - \sum_{m \in A_i} P_{i,m} \right) \\
 & + \sum_{m \in M} \mu_m \left(R_{RF,m} + R_{VLC,m}^{(k)} - R_{min} \right),
 \end{aligned}$$

subject to

$$P_{VLC,m} \leq P_{max}, \quad \forall m \in M \tag{10}$$

220 where $P_{max} = \min[(I_{DC} - I_{min})^2, (I_{max} - I_{DC})^2]$. The variables β^{RF} and β_i are the Lagrange prices of the maximum sum power constraints of the RF AP and VLC AP- i respectively. μ_m is the Lagrange price of the minimum rate constraint of MT- m . In order to decouple the RF part and the VLC part of the Lagrangian in (10), we set an initial value to μ_m , the Lagrange price of the minimum rate constraint of MT- m , for all $m \in M$ and update their values

²²⁵ using the gradient descent method as follows

$$\mu_m(t+1) = \left[\mu_m(t) - \epsilon(R_{RF,m} + R_{VLC,m}^{(k)} - R_{min}) \right]_+. \quad (11)$$

4.1.1. RF Power Allocation

The optimal RF power allocated to $MT-m$ is obtained by solving

$$\frac{\delta L}{\delta P_{RF,m}} = (1 + \mu_m) \frac{\delta R_{RF,m}}{\delta P_{RF,m}} - \lambda - \beta^{RF} = 0, \quad (12)$$

²³⁰ which can be obtained in a closed form as follows

$$P_{RF,m}^* = \left[\frac{B_{RF,m}(1 + \mu_m)}{(\lambda + \beta^{RF}) \log(2)} - \frac{No^{RF} B_{RF,m}}{G_{RF,m}} \right]_+. \quad (13)$$

The Lagrange price β^{RF} is updated using the gradient descent method as follows,

$$\beta^{RF}(t+1) = \left[\beta^{RF}(t) - \epsilon(P_{RF,max} - \sum_{m \in M} P_{RF,m}) \right]_+. \quad (14)$$

4.1.2. VLC Power Allocation

The optimal VLC power is allocated by maximizing the VLC part of the Lagrangian in (10) as shown in (15) to get $P_{i,m}^*$ for all $m \in M$ and $i \in V$. This maximization can be solved using the gradient method [49].

$$\max_{\{P_{VLC,m}\}_{m \in M}} \left(\sum_{m \in M} (1 + \mu_m) R_{VLC,m}^{(k)} + \sum_{i \in V} \beta_i (P_{VLC,max} - \sum_{l \in A_i} P_{VLC,l}) \right).$$

subject to

$$P_{VLC,m} \leq P_{max}, \quad m \in M \quad (15)$$

²⁴⁰ The Lagrange prices are then updated using the gradient descent method as follows

$$\beta_i(t+1) = \left[\beta_i(t) - \epsilon(P_{VLC,max} - \sum_{m \in A_i} P_{VLC,m}) \right]_+. \quad (16)$$

Since the VLC rates $R_{VLC}^{(k)}$ were defined at an arbitrary vector $\underline{P}_{VLC}^{(k)}$, this arbitrary vector needs to be iterated over for a number of iterations until convergence [46]. Algorithm 1 summarizes the RF/VLC power allocation.

Algorithm 1 RF/VLC Power Allocation

Initialize $\underline{P}_{VLC}^{(0)}$
Initialize $\lambda(0)$

- 1: **For** $k = 1 : K$
 - 2: **Set** $t = 0$
 - 3: **While** $F(\lambda(t)) \neq 0$ **Do**
 - 4: **Set** $\underline{\mu}$
 - 5: **Set** β^{RF}
 - 6: **Get** $P_{RF,m}^*$ from (13) for all $m \in M$
 - 7: **Update** $\beta^{RF} = [\beta^{RF} - \epsilon(P_{RF,max} - \sum_{m \in M} P_{RF,m}^*)]_+$
 - 8: **Repeat** from step 6 until convergence
 - 9: **Set** $\underline{\beta}$
 - 10: **Solve** (15) using gradient method to get $P_{VLC,m}^*$ for all $m \in M$
 - 11: **Update** $\beta_i = [\beta_i - \epsilon(P_{VLC,max} - \sum_{m \in A_i} P_{VLC,m})]_+$, $\forall i \in V$
 - 12: **Repeat** from step 10 until convergence
 - 13: **Update** $\mu_m = [\mu_m - \epsilon(R_{RF,m} + R_{VLC,m}^{(k)} - R_{min})]_+$, $\forall m \in M$
 - 14: **Repeat** from step 5 until convergence
 - 15: **Update** $\lambda(t+1) = \text{Power Efficiency}(t)$
 - 16: **Update** $t = t + 1$
 - 17: **End While**
 - 18: **Update** $\underline{P}_{VLC}^{(k)} = \underline{P}_{VLC}^*$
 - 19: **End For**
-

²⁴⁵ 4.2. RF/VLC Bandwidth Allocation

In this sub-problem, we consider the power allocation to be known and solve for the optimal bandwidth allocation. The bandwidth allocation has no effect on the denominator of the power efficiency objective in (4) (the total power

consumed by the system). Therefore, the denominator can be safely removed
250 from this sub-problem. The bandwidth allocation sub-problem is reduced to a sum rate maximization problem with maximum bandwidth and minimum user rate constraints. The problem is concave, and therefore can be solved using optimization software or using the KKT conditions. The Lagrangian of the BW allocation problem is

$$\begin{aligned} L = & \sum_{m \in M} (R_{RF,m} + R_{VLC,m}) + \alpha^{RF} \left(B_{RF} - \sum_{m \in M} B_{RF,m} \right) \\ & + \sum_{i \in V} \alpha_i \left(B_{VLC} - \sum_{m \in A_i} B_{i,m} \right) + \sum_{m \in M} \zeta_m (R_{RF,m} + R_{VLC,m} - R_{min}), \end{aligned} \quad (17)$$

255 where α^{RF} and α_i are the Lagrange prices of the maximum bandwidth constraints of the RF AP and VLC AP- i respectively. ζ_m is the Lagrange price of the minimum rate constraint of MT- m . Similarly, in order to decouple the RF part and the VLC part of the Lagrangian, we set an initial value to ζ_m , the Lagrange price of the minimum rate constraint of MT- m , for all $m \in M$ and
260 update their values using the gradient descent method as follows

$$\zeta_m(t+1) = [\zeta_m(t) - \epsilon(R_{RF,m} + R_{VLC,m} - R_{min})]_+. \quad (18)$$

The optimal RF bandwidth allocated to MT- m ($B_{RF,m}^*$) is the positive root of the equation

$$\frac{\delta L}{\delta B_{RF,m}} = (1 + \zeta_m) \frac{\delta R_{RF,m}}{\delta B_{RF,m}} - \alpha^{RF} = 0 \quad (19)$$

265 where $\frac{\delta R_{RF,m}}{\delta B_{RF,m}}$ is the first derivative of the RF rate of MT- m , and is given as

$$\frac{\delta R_{RF,m}}{\delta B_{RF,m}} = \left[\log_2 \left(1 + \frac{P_{RF,m} G_{RF,m}}{No^{RF} B_{RF,m}} \right) - \frac{P_{RF,m} G_{RF,m}}{\ln(2)(P_{RF,m} G_{RF,m} + No^{RF} B_{RF,m})} \right] \quad (20)$$

Similarly, the optimal VLC BW allocated to MT- m by its serving VLC AP

$(B_{VLC,m}^*)$ is the positive root of

$$\frac{\delta L}{\delta B_{VLC,m}} = (1 + \zeta_m) \frac{\delta R_{VLC,m}}{\delta B_{VLC,m}} - \alpha_{s(m)} = 0 \quad (21)$$

where $\frac{\delta R_{VLC,m}}{\delta B_{VLC,m}}$ is the first derivatives of the VLC rate of $MT-m$, and is given as follows

$$\begin{aligned} \frac{\delta R_{VLC}}{\delta B_{VLC,m}} &= \frac{1}{2} \left[\log_2 \left(1 + \frac{P_{VLC,m} G_{s(m),m}}{N o^{VLC} B_{s(m),m} + \Psi_m} \right) \right. \\ &\quad \left. - \frac{P_{VLC,m} G_{s(m),m} N o^{VLC} B_{VLC,m}}{\ln(2)(P_{VLC,m} G_{s(m),m} + N o^{VLC} B_{VLC,m} + \Psi_m)(N o^{VLC} B_{VLC,m} + \Psi_m)} \right] \end{aligned} \quad (22)$$

The above steps are summarized in algorithm2.

Algorithm 2 RF/VLC Bandwidth Allocation

- 1: **Initialize:** $\underline{\zeta}$
 - 2: **Set** α^{RF}
 - 3: **Solve** (19) for $B_{RF,m}^*$, $\forall m \in M$
 - 4: **Update** $\alpha^{RF} = [\alpha^{RF} - \epsilon(B_{RF,max} - \sum_{m \in M} B_{RF,m}^*)]_+$
 - 5: **Repeat** from step 3 until convergence
 - 6: **Set** $\underline{\alpha}$
 - 7: **Solve** (21) for $B_{VLC,m}^*$, $\forall i \in V, m \in A_i$
 - 8: **Update** $\alpha_i = [\alpha_i - \epsilon(B_{VLC,max} - \sum_{m \in A_i} B_{VLC,m}^*)]_+$, $\forall i \in V$
 - 9: **Repeat** from step 7 until convergence
 - 10: **Update** $\zeta_m = [\zeta_m - \epsilon(R_{RF,m} + R_{VLC,m} - R_{min})]_+$, $\forall m \in M$
 - 11: **Repeat** from step 2 until convergence
-

275 *4.3. Computational Complexity*

The computational complexity of JOBPA is of order I_{AO} times the total complexity of Algorithms 1 and 2, where I_{AO} is the number of iterations between the power and the bandwidth sub-problems [43]. Authors of [51] show that

the gradient method has a computational complexity that is polynomial in the
280 number of dual variable used. Therefore, the RF power allocation and the
VLC power allocation can be executed in parallel with complexity $O(MV)$.
The total computational complexity of Algorithm 1 is $O(I_{Db}(M + V)MVK)$,
where K is the number of iterations over the power vector \underline{P}^k , and I_{Db} is
the number of iterations required to find the roots of $F(\lambda)$. By analogy, the
285 computational complexity of Algorithm 2 can be estimated by $O((M + V)MV)$.
Therefore the total computational complexity of JOBPA can be estimated by
 $O(I_{AO}I_{Db}KVM(M + V))$.

5. Numerical Results

5.1. Simulation Setup

290 We consider a room of size (6m \times 6m \times 3m) with equally spaced 9 downward
pointing Luminaries. The luminaries are installed on the ceiling as shown in
Fig.3. Each LED luminary has the potential to work as a VLC AP besides its
main task as an illumination device. To achieve mean illuminance of 500 lux at
a desk level in the room [52], each luminary consists of 50 LEDs of type OSRAM
295 LCW W5SM [53] with half power angle of 60°. The illumination level contours
in the room is shown in Fig. 4. The LED has electrical to optical conversion
efficiency (k) of 0.54 W/A, a typical DC bias current (I_{DC}) of 350 mA, and
minimum and maximum driving currents (I_{min} and I_{max}) of 100 mA and 1 A,
respectively [53].

300 An RF AP is placed on a desk of height 1.6m and is separated from the
considered room by 3 heavy walls. The maximum bandwidth and power of the
RF AP ($B_{RF,max}$ and $P_{RF,max}$) are 10 MHz and 1 W [54],[34]. The maximum
bandwidth and power of each VLC AP ($B_{VLC,max}$ and $P_{VLC,max}$) are 20 MHz
and 1.3 W. The RF noise power spectral density is 3.89×10^{-21} W/Hz and the
305 VLC noise power spectral density is 10^{-21} W/Hz [34].

A number of $|M|$ MTs are located randomly in the room at four different
heights (0.6 m, 0.9 m, 1.1 m, and 1.7 m). The four heights stand for MTs on

a coffee table, MTs on a high desk, MTs with sitting people, and MT with standing people, respectively. The photo detector at the receiver of each MT has a field of view of 120° , a physical area of 1 cm^2 , and a responsivity (ρ) of 0.8 A/W.

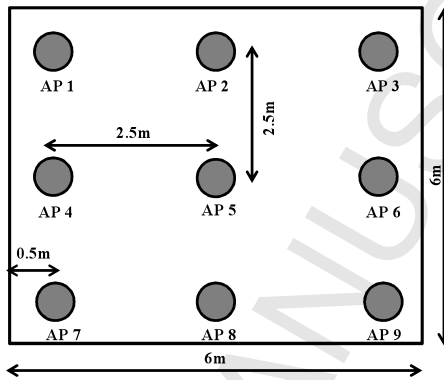


Figure 3: Locations of the LED Luminaries on the ceiling

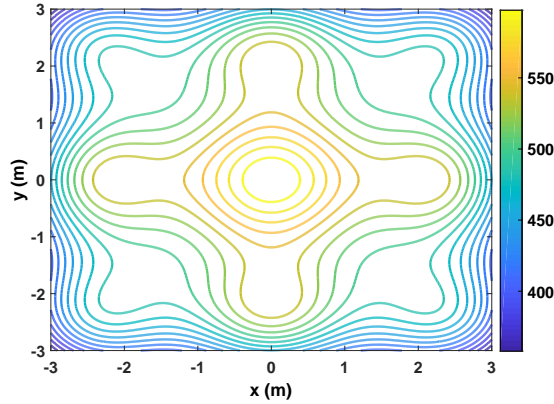


Figure 4: Contours of the illumination levels (lux)

5.2. Simulation Results

This subsection evaluates the power efficiency of the hybrid system. We study the system power efficiency in different layouts of the VLC APs. In all

³¹⁵ layouts, the RF AP serves all the MTs, and all the luminaries work as illumination devices. However, each layout allows a different group of Luminaries to operate as VLC APs besides their main illumination task. The following list shows the operating VLC APs in each layout.

- *Center*: the center luminary (AP 5)
- ³²⁰ • *Diag \:* the diagonal luminaries (APs 1,5,9)
- *Corners*: the corner luminaries (APs 1,3,7,9)
- *Shape ×*: the \times shaped luminaries (APs 1,3,5,7,9)
- *All Room*: all the luminaries (APs 1,2,3,...,9)

³²⁵ Figure 5 compares the power efficiency of different layouts of the VLC APs. The power efficiency is calculated for eight users in the room and at different minimum rate requirements (R_{min}) ranging from 2.5 Mbps to 20 Mbps per user. The figure shows that increasing the number of the VLC AP in the room increases the power efficiency for all the calculated values of R_{min} thanks to reusing the VLC band. Increasing the minimum rate requirements (R_{min}) motivates the APs to allocate more power and to distribute it less opportunistically among their associated users, and therefore the power efficiency decreases as the minimum per user rate required increases. Increasing R_{min} affects the power efficiency of layouts with many VLC APs (e.g. *All Room* and *Shape ×*) more than other scenarios due to the increased inter AP interference.

³³⁵ Figure 6 shows what percentage of the total system rate achieved by the VLC APs. The VLC systems contribute more than 50% of the total rate even in layout *Center* which has a single VLC AP. Increasing the number of VLC APs layouts increases the VLC rate contribution. Also it is noticeable that the VLC contribution decreases by increasing the minimum rate requirement. ³⁴⁰ Therefore we can conclude that most users depend on the power efficient VLC to satisfy their rate requirement, and that increasing the number of VLC APs reduces the dependence on the RF system.

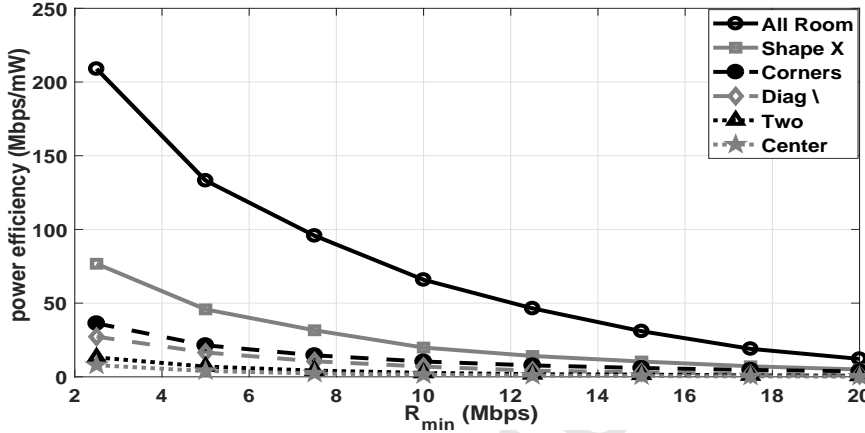


Figure 5: Power efficiency for different minimum rate requirements (R_{min}) (at $|M|=8$ users)

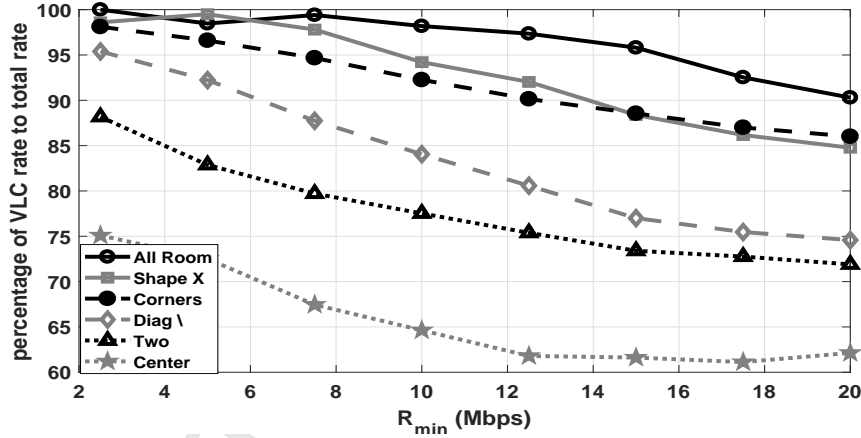


Figure 6: Percentage of VLC rate to total rate for different minimum rate requirements (R_{min}) (at $|M|=8$ users)

Similarly, Fig. 7 shows the power efficiency of different VLC AP layouts calculated for different number of users at minimum rate requirement of 10 Mbps. Again, the power efficiency decreases as the number of users in the room increases because it has to satisfy the QoS requirement of the new users. Layout *All Room* has higher power efficiency, but it is the fastest to drop due to the increased inter AP interference. Figure 8 shows that the VLC system

contributes the major portion of the hybrid system's rate. As the number of users increase, the RF contribution increases to help support more users.
 350

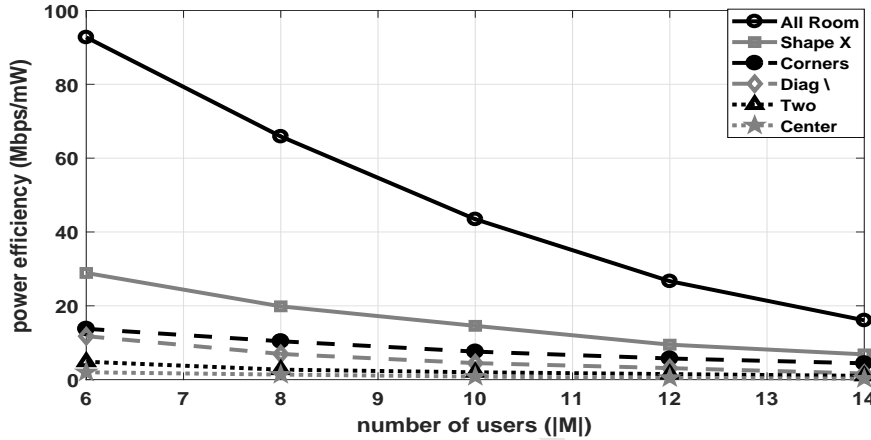


Figure 7: Power Efficiency for different number of users $|M|$ (at $R_{min}=10$ Mbps)

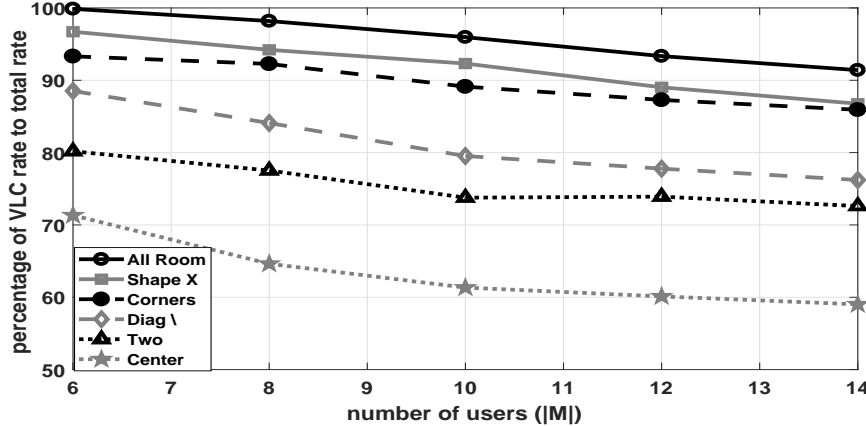


Figure 8: Percentage of VLC rate to total rate for different number of users $|M|$ (at $R_{min}=10$ Mbps)

Figure 9 shows the effect of changing the receiver's field of view (FOV) on the power efficiency of different VLC AP layouts. The power efficiencies are calculated for eight users in the room and at R_{min} of 10 Mbps. Reducing the receiver's FOV reduces the power efficiency as it makes more users out of the

355 coverage of the VLC APs and therefore the system depends more on the RF coverage as shown in Fig.10. The figure shows that the contribution of the VLC system to the total achieved rate decreases when decreasing the receiver's FOV, especially in Layouts with sparse VLC APs like layout *Two*.

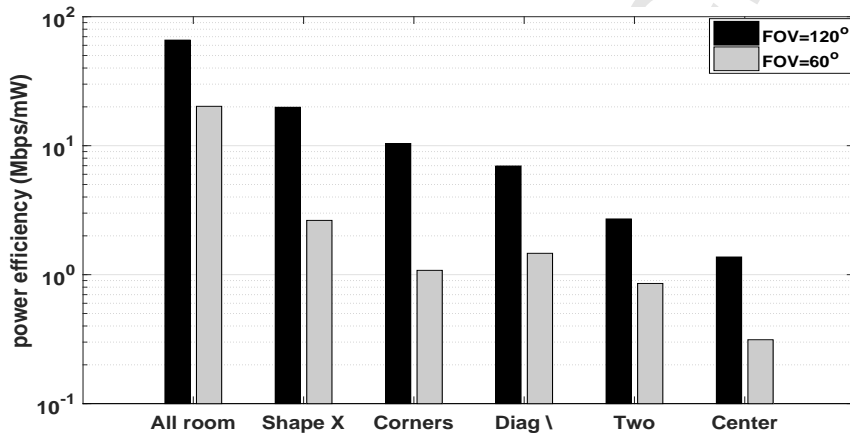


Figure 9: Power efficiency of different layouts at $\text{FOV}=120^\circ$ and 60° (at $R_{\min}=10$ Mbps and $|M|=8$ users)

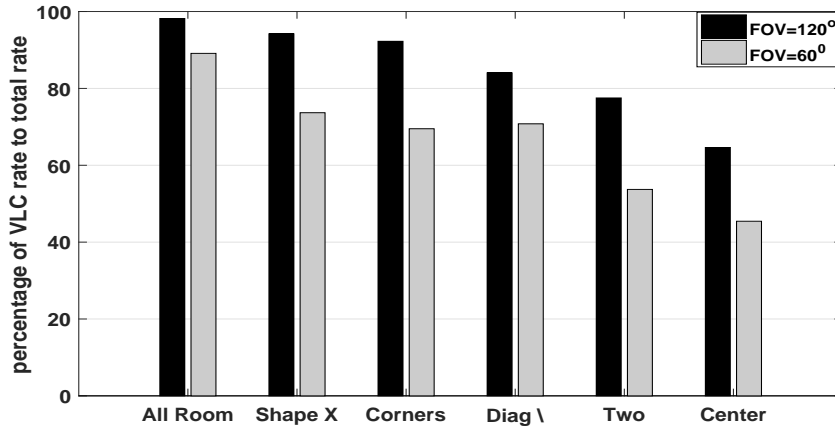


Figure 10: Percentage of VLC rate to total rate for different layouts at $\text{FOV}=120^\circ$ and 60° (at $R_{\min}=10$ Mbps and $|M|=8$ users)

6. Summary and Conclusions

360 This paper focuses on evaluating the power efficiency of the hybrid RF/VLC system. The power efficiency is defined as the system's total rate divided by the total power consumed, and is measured in bps/W. We consider an indoor system consisting of a room with a number of LED luminaries installed on the ceiling and working as interfering VLC access points (APs). An RF AP is located 365 outside the room. This model is valid for many scenarios.

A joint bandwidth and power allocation iterative algorithm was proposed to maximize the power efficiency of the system while satisfying maximum RF/VLC power and bandwidth constraints (taking into consideration the finite linear range of the deployed LEDs) along with minimum per user rate constraints.

370 Results show that deploying VLC with RF communication improves the power efficiency of the system, and that the hybrid RF/VLC system mainly depends on the VLC to provide the users with their required rate as it is more power efficient. The dependency on the RF communication system only increases when the number of users increases or when the minimum rate required 375 per user increases.

7. Acknowledgement

This publication was made possible by the NPRP project # 9-077-2-036 from the Qatar National Research Fund (a member of The Qatar Foundation). The statements made herein are solely the responsibility of the author[s].

380 **References**

- [1] M. Cole, T. Driscoll, The lighting revolution: If we were experts before, we're novices now, in: the 59th conference on Petroleum and Chemical Industry Technical Conference (PCIC), 2012, pp. 1–12. doi:10.1109/PCICON.2012.6549687.

- 385 [2] P. H. Pathak, X. Feng, P. Hu, P. Mohapatra, Visible light communication, networking, and sensing: A survey, potential and challenges, *IEEE communications surveys & tutorials* 17 (4) (2015) 2047–2077. doi:10.1109/COMST.2015.2476474.
- 390 [3] S. Dimitrov, H. Haas, *Principles of LED Light Communications: Towards Networked Li-Fi*, Cambridge University Press, 2015.
- [4] S. Rajagopal, R. D. Roberts, S.-K. Lim, IEEE 802.15. 7 visible light communication: modulation schemes and dimming support, *IEEE Communications Magazine* 50 (3) (2012) 72–82. doi:10.1109/MCOM.2012.6163585.
- 395 [5] S. Wu, H. Wang, C.-H. Youn, Visible light communications for 5G wireless networking systems: from fixed to mobile communications, *IEEE Network* 28 (6) (2014) 41–45. doi:10.1109/MNET.2014.6963803.
- [6] S. Zvanovec, P. Chvojka, P. A. Haigh, Z. Ghassemlooy, Visible light communications towards 5G, *Radioengineering* 24 (1) (2015) 1–9. doi:10.13164/re.2015.0001.
- 400 [7] M. B. Rahaim, A. M. Vigni, T. D. Little, A hybrid radio frequency and broadcast visible light communication system, in: *IEEE GLOBECOM Workshops (GC Wkshps)*, 2011, pp. 792–796. doi:10.1109/GLOCOMW.2011.6162563.
- 405 [8] R. Zhang, J. Wang, Z. Wang, Z. Xu, C. Zhao, L. Hanzo, Visible light communications in heterogeneous networks: Paving the way for user-centric design, *IEEE Wireless Communications* 22 (2) (2015) 8–16. doi:10.1109/MWC.2015.7096279.
- 410 [9] M. Ayyash, H. Elgala, A. Khreishah, V. Jungnickel, T. Little, S. Shao, M. Rahaim, D. Schulz, J. Hilt, R. Freund, Coexistence of WiFi and LiFi toward 5G: concepts, opportunities, and challenges, *IEEE Communications Magazine* 54 (2) (2016) 64–71. doi:0.1109/MCOM.2016.7402263.

- [10] L. Feng, R. Q. Hu, J. Wang, P. Xu, Y. Qian, Applying VLC in 5G networks: Architectures and key technologies, *IEEE Network* 30 (6) (2016) 77–83. doi:10.1109/MNET.2016.1500236RP.
- 415 [11] I. Stefan, H. Burchardt, H. Haas, Area spectral efficiency performance comparison between VLC and RF femtocell networks, in: International Conference on Communications (ICC), 2013, pp. 3825–3829. doi:10.1109/ICC.2013.6655152.
- 420 [12] J. Grubor, O. Jamett, J. Walewski, S. Randel, K. Langer, High-speed wireless indoor communication via visible light, in: ITG-Fachbericht-Breitbandversorgung in Deutschland-Vielfalt für alle?, 2007, pp. 203–208.
- [13] C. Chen, D. A. Basnayaka, H. Haas, Downlink performance of optical atocell networks, *J. Lightwave Technol.* 34 (1) (2016) 137–156.
- 425 [14] M. Kashef, M. Abdallah, K. Qaraqe, H. Haas, M. Uysal, On the benefits of cooperation via power control in OFDM-based visible light communication systems, in: the 25th International Symposium on Personal, Indoor, and Mobile Radio Communication (PIMRC), 2014, pp. 856–860. doi:10.1109/PIMRC.2014.7136285.
- 430 [15] M. Kashef, M. Abdallah, K. Qaraqe, M. Uysal, The impact of location errors on achievable rates in OFDM-based multi-user visible light communication systems, in: the 3rd International Workshop in Optical Wireless Communications (IWOW), 2014, pp. 65–69. doi:10.1109/IWOW.2014.6950778.
- 435 [16] C. Chen, D. Tsonev, H. Haas, Joint transmission in indoor visible light communication downlink cellular networks, in: IEEE GLOBECOM Workshops (GC Wkshps), 2013, pp. 1127–1132. doi:10.1109/GLOCOMW.2013.6825144.
- [17] F. Jin, X. Li, R. Zhang, C. Dong, L. Hanzo, Resource allocation under

- A
C
C
P
T
E
D
S
C
R
I
P
T
- delay-guarantee constraints for visible-light communication, *IEEE Access* 4 (2016) 7301–7312. doi:10.1109/ACCESS.2016.2564298.
- [18] A. M. Abdelhady, O. Amin, A. Chaaban, M.-S. Alouini, Downlink resource allocation for multichannel TDMA visible light communications, in: Global Conference on Signal and Information Processing (GlobalSIP), 2016, pp. 1–5. doi:10.1109/GlobalSIP.2016.7905771.
- [19] H. Liu, H. Dai, Y. Chen, P. Xia, Conflict graph-based downlink resource allocation and scheduling for indoor visible light communications, *Journal of the Optical Society of Korea* 20 (1) (2016) 36–41.
- [20] X. Li, R. Zhang, L. Hanzo, Cooperative load balancing in hybrid visible light communications and WiFi, *IEEE Transactions on Communications* 63 (4) (2015) 1319–1329. doi:10.1109/TCOMM.2015.2409172.
- [21] Y. Wang, H. Haas, Dynamic load balancing with handover in hybrid LiFi and WiFi networks, *J. Lightwave Technol.* 33 (22) (2015) 4671–4682.
- [22] L. Li, Y. Zhang, B. Fan, H. Tian, Mobility-aware load balancing scheme in hybrid VLC-LTE networks, *IEEE Communications Letters* 20 (11) (2016) 2276–2279. doi:0.1109/LCOMM.2016.2598559.
- [23] Y. Wang, X. Wu, H. Haas, Load balancing game with shadowing effect for indoor hybrid LiFi/RF networks, *IEEE Transactions on Wireless Communications* 16 (4) (2017) 2366–2378. doi:10.1109/TWC.2017.2664821.
- [24] X. Bao, X. Zhu, T. Song, Y. Ou, Protocol design and capacity analysis in hybrid network of visible light communication and OFDMA systems, *IEEE Transactions on Vehicular Technology* 63 (4) (2014) 1770–1778. doi:10.1109/TVT.2013.2286264.
- [25] J. Hou, D. C. O'Brien, Vertical handover decision making algorithm using fuzzy logic for the integrated radio and OW system, *IEEE Transactions on Wireless Communications* 5 (1) (2006) 176–185. doi:10.1109/TWC.2006.1576541.

- [26] I. Stefan, H. Haas, Hybrid visible light and radio frequency communication systems, in: Vehicular Technology Conference (VTC Fall), 2014, pp. 1–5. doi:10.1109/VTCFall.2014.6965999.
- ⁴⁷⁰ [27] J. Wang, C. Jiang, H. Zhang, X. Zhang, V. C. Leung, L. Hanzo, Learning-aided network association for hybrid indoor LiFi-WiFi systems, IEEE Transactions on Vehicular Technology (99) (2017) –. doi:10.1109/TVT.2017.2778345.
- ⁴⁷⁵ [28] H. Tabassum, E. Hossain, Coverage and rate analysis for co-existing RF/VLC downlink cellular networks, IEEE Transactions on Wireless Communications (99) (2018) –. doi:10.1109/TWC.2018.2799204.
- [29] D. A. Basnayaka, H. Haas, Design and analysis of a hybrid radio frequency and visible light communication system, IEEE Transactions on Communications 65 (10) (2017) 4334–4347. doi:10.1109/TCOMM.2017.2702177.
- ⁴⁸⁰ [30] M. Ismail, W. Zhuang, Network cooperation for energy saving in green radio communications, IEEE Wireless Communications 18 (5) (2011) 76–81. doi:10.1109/MWC.2011.6056695.
- ⁴⁸⁵ [31] S. McLaughlin, P. M. Grant, J. S. Thompson, H. Haas, D. I. Laurenson, C. Khirallah, Y. Hou, R. Wang, Techniques for improving cellular radio base station energy efficiency, IEEE Wireless Communications 18 (5) (2011) 10–17. doi:10.1109/MWC.2011.6056687.
- [32] H. Haas, LiFi is a paradigm-shifting 5G technology, Reviews in Physics 3 (2017) 26–31. doi:10.1016/j.revip.2017.10.001.
- ⁴⁹⁰ [33] S. Ma, T. Zhang, S. Lu, H. Li, Z. Wu, S. Li, Energy efficiency of SISO and MISO in visible light communication systems, Journal of Lightwave Technology (99) (2018) –. doi:10.1109/JLT.2018.2812831.
- [34] M. Kashef, M. Ismail, M. Abdallah, K. A. Qaraqe, E. Serpedin, Energy efficient resource allocation for mixed RF/VLC heterogeneous wireless net-

- works, IEEE Journal on Selected Areas in Communications 34 (4) (2016) 883–893. doi:10.1109/JSAC.2016.2544618.
- [35] M. Kashef, M. Abdallah, N. Al-Dahir, Transmit power optimization for a hybrid PLC/VLC/RF communication system, IEEE Transactions on Green Communications and Networking 2 (1) (2018) 234 – 245. doi:10.1109/TGCM.2017.2774104.
- [36] R. Zhang, H. Claussen, H. Haas, L. Hanzo, Energy efficient visible light communications relying on amorphous cells, IEEE Journal on Selected Areas in Communications 34 (4) (2016) 894–906. doi:10.1109/JSAC.2016.2544598.
- [37] D1.1.2 v1.2 WINNER II channel models, last accessed on 19/3/2017 (2008). URL <https://cept.org/files/8339/winner2%20-%20final%20report.pdf>
- [38] L. Zeng, D. C. O'Brien, H. Le Minh, G. E. Faulkner, K. Lee, D. Jung, Y. Oh, E. T. Won, High data rate multiple input multiple output (MIMO) optical wireless communications using white LED lighting, IEEE Journal on Selected Areas in Communications 27 (9) (2009) 1654 – 1662. doi:10.1109/JSAC.2009.091215.
- [39] L. Yin, W. O. Popoola, X. Wu, H. Haas, Performance evaluation of non-orthogonal multiple access in visible light communication, IEEE Transactions on Communications 64 (12) (2016) 5162–5175. doi:10.1109/TCOMM.2016.2612195.
- [40] J. R. Barry, J. M. Kahn, W. J. Krause, E. A. Lee, D. G. Messerschmitt, Simulation of multipath impulse response for indoor wireless optical channels, IEEE journal on selected areas in communications 11 (3) (1993) 367–379. doi:10.1109/49.219552.
- [41] R. C. Kizilirmak, C. R. Rowell, M. Uysal, Non-orthogonal multiple access (NOMA) for indoor visible light communications, in: International

- Workshop on Optical Wireless Communications (IWOW), 2015, pp. 98–101. doi:10.1109/IWOW.2015.7342274.
- [42] B. Ghimire, H. Haas, Self-organising interference coordination in optical wireless networks, EURASIP Journal on Wireless Communications and Networking 2012 (1) (2012) 1–15. doi:10.1186/1687-1499-2012-131.
- [43] L. Grippo, M. Sciandrone, On the convergence of the block nonlinear gauss-seidel method under convex constraints, Operations research letters 26 (3) (2000) 127–136. doi:10.1016/S0167-6377(99)00074-7.
- [44] A. Zappone, E. Jorswieck, et al., Energy efficiency in wireless networks via fractional programming theory, Foundations and Trends® in Communications and Information Theory 11 (3-4) (2015) 185–396. doi:10.1561/0100000088.
- [45] J.-P. Crouzeix, J. A. Ferland, Algorithms for generalized fractional programming, Mathematical Programming 52 (1-3) (1991) 191–207. doi:10.1007/BF01582887.
- [46] H. H. Kha, H. D. Tuan, H. H. Nguyen, Fast global optimal power allocation in wireless networks by local DC programming, IEEE Transactions on Wireless Communications 11 (2) (2012) 510–515. doi:10.1109/TWC.2011.120911.110139.
- [47] S. Schaible, Fractional programming, Zeitschrift für Operations-Research 27 (1) (1983) 39–54. doi:10.1007/BF01916898.
- [48] M. Grant, S. Boyd, Y. Ye, CVX: Matlab software for disciplined convex programming (2008).
- URL <http://cvxr.com/cvx/>
- [49] S. Boyd, L. Vandenberghe, Convex optimization, Cambridge university press, 2004.

- [50] H. Hindi, A tutorial on convex optimization II: duality and interior point methods, in: American Control Conference, 2006, pp. 11–18. doi:10.1109/ACC.2006.1655436.
- [51] M. S. Alam, J. W. Mark, X. S. Shen, Relay selection and resource allocation for multi-user cooperative OFDMA networks, IEEE Transactions on Wireless Communications 12 (5) (2013) 2193–2205. doi:10.1109/TWC.2013.032113.120652.
- [52] illumination requirements, last accessed 19/3/2018.
URL <http://www.gsa.gov/portal/content/101308>
- [53] Datasheet: LCW W5SM Golden Dragon,white led, last accessed 19/3/2018.
URL <https://www.osram.com/os/index.jsp>
- [54] I. Ashraf, F. Boccardi, L. Ho, Sleep mode techniques for small cell deployments, IEEE Communications Magazine 49 (8) (2011) 72–79. doi:10.1109/MCOM.2011.5978418.

Mai Kafafy

Mai Kafafy received the M.Sc and B.Sc. in Electronics and Communications Engineering from Cairo University in 2014 and 2011, respectively. She is currently working on her PhD in Cairo University. Her current research interests include wireless communications and visible light communications.

Yasmine Fahmy

Dr. Yasmine A. H. Fahmy received the B.Sc with honors in 1999 where she graduated as top of her class, the MSc. in 2001, and the PhD. in 2005, all in telecommunications, and all from the faculty of Engineering at Cairo University. She is presently an associate professor at the Electronics and Communications Department, Faculty of Engineering, Cairo University. Her current research field of interest includes wireless communication, modern coding techniques and MIMO systems.

Mohamed Abdallah

Mohamed Abdallah was born in Giza, Egypt. He received his B.Sc degree from Cairo University in 1996. He received his M. Sc. and Ph.D. degrees from the University of Maryland at College Park in 2001 and 2006, respectively. From 2006 to 2016, he held academic and research positions at Cairo University and Texas A&M University at Qatar. Currently, he is a founding faculty member with the rank of Assistant Professor at College of Science and Engineering at Hamad bin Khalifa University (HBKU). His current research interests include the design and performance of physical layer algorithms for cognitive networks, cellular heterogeneous networks, sensor networks, smart grids, visible light and free-space optical communication systems, and reconfigurable smart antenna systems. Dr. Abdallah is the recipient of the Research Fellow Excellence Award at Texas A&M University at Qatar in 2016, the best paper award in the IEEE First Workshop on Smart Grid and Renewable Energy in 2015, and the Nortel Networks Industrial Fellowship for five consecutive years, 1999-2003. Dr. Abdallah professional activities include an associate editor for IEEE Transactions on Communications, a technical program chair of the 10th International Conference on Cognitive Radio Oriented Wireless Networks, and a technical program committee member of several major IEEE conferences.

Mohamed Khairy

Mohamed Khairy received his BSc degree (valedictorian) and his MSc degree from Cairo University, Cairo, Egypt, in 1992 and 1995, respectively, and his MSc degree and his PhD degree all in electrical engineering from the University of Maryland, College Park, MD, USA, in 1997 and 2000, respectively.

Since 2001, he has been with the Department of Electronics and Communications at Cairo University, where he is currently a professor. He supervised over than 30 MSc theses. He is also the IEEE Egypt section vice president. From 1995 to 2002, he consulted for LCC Inc., Philips Research Labs, Orbital Sciences, Ellipsis digital systems, and SySDsoft.

Dr Khairy was the first author of a paper that won the Best Paper Award at the IEEE Fifth International Symposium on Spread Spectrum Techniques and Applications in 1998. He has authored and co-authored more than 60 papers in the areas of coding, modulation, CDMA,

OFDM, space-time codes and cross-layer design among other areas. He also holds and applied for several patents in these areas.

Dr Khairy is also the founder and director of the Center for Wireless studies at Cairo University. The Center for Wireless Studies (CWS) was established to streamline the technical research effort in the communication system design and implementation within the university.

Mai Kafafy



Yasmine Fahmy



Mohamed Abdallah



Mohamed Khairy

